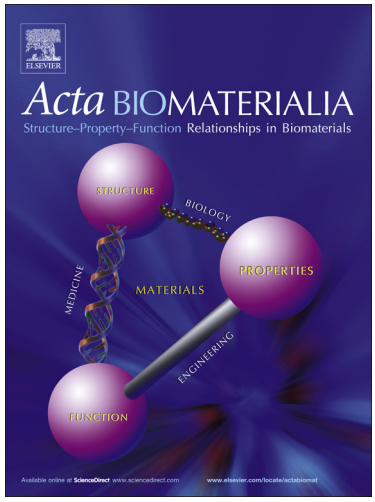

3D bioprinted extracellular matrix mimics facilitate directed differentiation of epithelial progenitors for sweat gland regeneration

Sha Huang, Bin Yao, Jiangfan Xie, Xiaobing Fu

PII: S1742-7061(15)30276-2
DOI: http://dx.doi.org/10.1016/j.actbio.2015.12.039
Reference: ACTBIO 4053

To appear in: *Acta Biomaterialia*

Received Date: 15 July 2015
Revised Date: 10 December 2015
Accepted Date: 30 December 2015

Please cite this article as: Huang, S., Yao, B., Xie, J., Fu, X., 3D bioprinted extracellular matrix mimics facilitate directed differentiation of epithelial progenitors for sweat gland regeneration, *Acta Biomaterialia* (2015), doi: http://dx.doi.org/10.1016/j.actbio.2015.12.039

Title Page

3D bioprinted extracellular matrix mimics facilitate directed differentiation of epithelial progenitors for sweat gland regeneration

Sha Huang, MD, Ph.D.,[1,2,3*†] Bin Yao, M.M.,[1*] Jiangfan Xie, M.M.,[1,4] Xiaobing Fu, MD, Ph.D.[1†]

1 Key Laboratory of Tissue Repair and Regeneration of PLA, and Beijing Key Research Laboratory of Skin Injury, Repair and Regeneration, First Hospital Affiliated to General Hospital of PLA, Beijing 100048, PR China;

2 Institute of Basic Medical Sciences, General Hospital of PLA, Beijing 100853, P. R. China

3 Hainan Branch of the Chinese PLA General Hospital, Sanya 572014, P. R. China

4 Graduate School of Tianjin Medical University, Tianjin, 300052, P.R. China

*** These authors contributed equally to this work.**

† Correspondence should be addressed to:

Xiaobing Fu, MD, PhD; Sha Huang, MD, Ph.D.

Key Laboratory of Tissue Repair and Regeneration of PLA

The First Affiliated Hospital

General Hospital of PLA

51 Fu Cheng Road, Beijing 100048 P. R. CHINA

Fax: 0086 10 68989955

e-mail: *fuxiaobing@vip.sina.com; stellarahuang@sina.com*

Abstract

Sweat glands perform a vital thermoregulatory function in mammals. Like other skin appendages, they originate from epidermal progenitors. However, they have low regenerative potential in response to injury, and whether adult epidermal progenitors could be specified to differentiate to a sweat gland cell lineage remains largely unexplored. We used bioprinting technology to create a functional *in vitro* cell-laden 3D extracellular matrix mimics (3D-ECM) with composite hydrogels based on gelatin and sodium alginate because of chemical and structural similarity to ECM components. To achieve specific cell differentiation, mouse plantar dermis and epidermal growth factor were synchronously incorporated into the 3D-ECM mimics to create an inductive niche for epidermal progenitor cells obtained from mice. The biological 3D construct could maintain cell viability, thereby facilitating cell spreading and matrix formation. *In vitro* data by immunofluorescence and gene expression assay of key cell-surface markers demonstrated that the bioprinted 3D-ECM could effectively create a restrictive niche for epidermal progenitors that ensures unilateral differentiation into sweat gland cells. Furthermore, direct delivery of bioprinted 3D-ECM into burned paws of mice resulted in functional restoration of sweat glands. This study represents the rational design to enhance the specific differentiation of epidermal lineages using 3D bioprinting and may have clinical and translational implications in regenerating sweat glands.

Keywords: Bioprinting; extracellular matrix; epithelial progenitor; cell differentiation; sweat gland regeneration

INTRODUCTION

Body temperature is primarily controlled by sweating in mammals. Therefore, absent or malfunctioning sweat glands in hot climates, during physical exercise or fever can lead to hyperthermia, stroke, and even death [1, 2]. Heat intolerance also occurs survivors of large-scale deep burns even though the skin is restored, because severe skin burns may cause failure of complete sweat gland regeneration under hypertrophic scars [3]. Recent research has identified stem cell populations within the sweat glands in mouse paw pads and an active role of these cells in wound repair [4]. However, little is known about the molecular mechanisms of sweat gland activity and how local sweat gland cells are repaired when skin undergoes burns, wounds or chemical treatment. In these cases, the overall tissue architecture involving sweat glands must be severely disrupted, and undamaged sweat gland cells adjacent to the wound display a quiescent feature during skin wound repair, which poses a challenge for restitution of lost cells during wound healing.

Sweat glands, like other skin appendage cells, develop from the embryonic epidermis. However, in contrast to relatively well-characterized hair-follicle or other epidermal derivatives, much less is known about inductive niches of sweat glands. Epithelial-derived stem/progenitor cells represent promising candidates for regenerating sweat glands [5, 6], but the multiple-fate plasticity of these cells seems to be an intractable problem. Given these findings, unidentified regional dermal components and growth factors in extracellular matrix (ECM) may be vital for epithelial cell–fate determination. Moreover, the inductive power of ECM underlying epithelia was underscored by transplanting epithelial-derived sweat gland progenitors

in dorsal skin of mice: progenitors generated a stratified epidermis rather than sweat glands [4].

To provide better inductive cues for sweat gland regeneration, precise and instructive microenvironments for governing epidermal progenitor behaviors is of major importance. However, embryonic tissue application in these previous works on the regeneration of the sweat glands seems to be an insurmountable obstacle for translation to clinical practice. Recent studies of sweat gland development and homeostasis highlight that adult local tissues can ensure the behavior of epidermal progenitors and have inductive powers on sweat gland specification [4, 7]. Although further experiments are needed, use of adult tissue and cells is considered feasible for regenerating sweat glands. Besides dermal components, epidermal growth factor (EGF) has been implicated in the control of the epithelial cell phenotype [8] and seems to be an important regulator in the development of sweat glands [5].

In this context, creating a complex ECM comprising dermal components and EGF encircling cells and arranged in a three-dimensional pattern remains challenging. 3D bioprinting technology has high potential in providing accurate and organized *in vitro* simulation of stem cell niche [9]. It could also be beneficial for guiding tissue regeneration *in vivo* [10,11]. Furthermore, in terms of clinical application, delivering living cells with appropriate material in a defined and organized manner, in sufficient numbers, and within the right environment, with the use of 3D bioprinting, offers significant advantages.

Here we applied a bioprinting method for creating a cell-laden 3D-ECM capable

of providing an optimized microenvironment for specific differentiation of epithelial-derived stem or progenitor cells, with the cells and ECM components arranged in a defined spatial pattern. Moreover, as an adapted printing material, hydrogel make it possible to present several bioactive cues simultaneously and promote tissue regeneration in biomimetic fashion [12,13]. The bioprinted 3D-ECM mimics with organized patterns of mouse plantar dermis (PD) components and EGF within composite gelatin and sodium alginate hydrogels yielded crucial cues for the effective and accurate specific differentiation of mouse dorsal epithelial progenitors *in vitro* and *in vivo*. Our 3D-ECM matrix can enhance the feasibility and applicability of regenerating sweat glands in the clinic.

METHODS

Study design

This study was designed to determine whether epithelial-derived stem/progenitor cells can be differentiated effectively and specifically to regenerate sweat glands in the clinic. The primary parameters included 1) characterization of an *in vitro* 3D-ECM; 2) ECM synthesis and release efficiency of growth factors (EGF, bone morphogenetic protein 4 [BMP-4]), which are potent epidermal inducers of cell-fate determination [14]; 3) differentiation capacity of epithelial-derived stem/progenitor cells at gene and protein levels *in vitro*; and 4) functional analysis of epithelial-derived sweat glands *in vivo* (Fig. 1A).

Epithelial progenitor isolation from mouse dorsal skin

From female green fluorescent protein (GFP)-based C57/B16 mice (Jackson Laboratory) aged 3-4 weeks as described [15], epithelial progenitors were isolated from the dorsal basal epidermis. Skin samples were cut into small pieces, then centrifuged, and fat droplets were removed with the supernatant. Samples were digested with trypsin (Gibco) and trypsin-neutralized by adding DMEM medium (Gibco) supplemented with 2% fetal calf serum (FCS), and epidermis was completely digested from the dermis. Basal cells were mechanically separated from the epidermis by flushing 10 times under the epidermis. Obtained epithelial progenitors were incubated and further expanded during passage 1. Cells were grown in a serum-free medium (Invitrogen, containing 25 mg/ml bovine pituitary extract).

Dermal homogenates from mouse PD

From wild-type C57/B16 mice (Huafukang Co., Beijing) aged 5 days old, dermal homogenates were prepared by homogenizing freshly collected hairless mouse PD with isotonic phosphate buffer (IPB, pH=7.4) for 20 min in an ice bath to obtain 25% (w/v) tissue suspension. The supernatant was obtained after centrifugation at 4 °C for 20 min at 10000×g. Dermal homogenates from mouse dorsal dermis (DD) were collected as a control. BMP-4 plays important roles in epidermal fate guidance [16-18]. Hence, we performed western blot analysis of BMP-4 protein level with both PD and DD homogenates by use of a BMP-4 monoclonal antibody (Sigma) following the manufacturer's protocol.

Design and synthesis of *in vitro* 3D-ECM

The designed 3D-ECM was created by use of a bioprinting platform (Regenovo 3D

Bio-printer, China) based on rapid prototyping technology, which demonstrated its capability of printing live cells and biomaterials in designated places to form complex 3D structures [19]. A software interface (Microsoft, AT6400) enables on-demand printing of spatial patterns of the materials in 3D at cellular accuracy.

With the designed structure, a refit nozzle (0.2 mm) controlled by a computer was used to deposit the mixture on a glass chip at 10°C (gelatin at gel state). Briefly, a 4:1 mixture (200 μl) of suspended cells (culture media contained 15 ng/ml recombinant mouse EGF) and homogenates was added into a 2:1 mixture (5 ml) of 20% (w/v, polymer weight/solvent volume) gelatin (Sigma, 96 kDa, type B) and 4% sodium alginate (Sigma, 75–100 kDa, guluronic acid 39%) composite hydrogels (alginate sodium and gelatin were dissolved in phosphate buffered saline (PBS) respectively to form a homogeneous solution with a concentration of 4% or 20%), then loaded into a sterilized syringe and printed in a square in a criss-cross pattern. The final cell density in the bioprinted mixture was 0.2 million cells per mL. The program was run 4 times consecutively in the same position to generate a 3D configuration with the square pattern.

The designed 3D-ECM samples was bioprinted as 6 groups: control (only epithelial progenitor-laden composite hydrogels); Eps+EGF (epithelial progenitors with EGF-laden composite hydrogels); Eps+PD+EGF (epithelial progenitors with PD homogenate-laden composite hydrogels with EGF) and Eps+PD (epithelial progenitors with PD homogenate-laden composite hydrogels without EGF); Eps+DD+EGF (epithelial progenitors with DD homogenate-laden composite

hydrogels with EGF) and Eps+DD (epithelial progenitors with DD homogenate-laden composite hydrogels without EGF).

When the process was finished, the 3D-ECM structure was cross-linked with 10% $CaCl_2$ for 1 min (to crosslink the alginate) and washed with DMEM 3 times. Non–cross-linked bioprinted 3D-ECM was fabricated as a control. Bioprinted 3D-ECM samples were further stabilized in a culture medium containing DMEM, 10% FCS, 1 mmol/L insulin, and placed in a CO_2 incubator at 37°C. After 24 to 72 h, bioprinted 3D-ECM samples were observed by fluorescence microscopy (Leica BMI4000, Germany). Some samples were dried in a vacuum freeze dryer for 12 h. After dehydration, bioprinted 3D-ECM samples were sputter coated with gold–palladium and observed by scanning electron microscopy (SEM; Hitachi S480, Japan).

Cell viability and growth factor delivery

After 1 to 7 days of incubation, viability of cells were determined by MTS assay (CellTiter 96, Promega, USA). Cells harvested from bioprinted 3D-ECM samples were observed under a microscope (Leica BMI4000, Germany) at various times.

The medium was changed every other day, and supernatant was collected from the incubation solution for the bioprinted 3D-ECM samples. Released EGF and BMP-4 content was measured by use of ELISA kits (ABIN ABIN424243; ABIN1568654; Antibodies-online.cn, Aachen, Germany).

***In vitro* differentiation assay**

The bioprinted 3D-ECM samples were fixed with a solution of 4% paraformaldehyde

after 14 days' culture, then embedded in OCT compound and sectioned at 8-mm thickness. For visualizing differentiation, sections were immunostained with primary anti-cytokeratin antibodies (epidermal basal cell cytokeratins CK5 and CK14 and sweat gland luminal cytokeratins CK8 and CK18; Abcam, USA) following the manufacturer's protocol, then secondary goat anti-rabbit antibody (1:100; Invitrogen, CA), with counterstaining with DAPI. Stained images were visualized by confocal microscopy (Leica TCS SP8).

To detect genetic differentiation, total RNA of cells harvested from bioprinted 3D-ECM samples was isolated by use of TRIzol reagent (Invitrogen Life Technologies, USA) after 14 days' culture. RNA concentration was measured by use of Nanodrop (Thermo Scientific, USA). Reverse transcription involved a cDNA synthesis kit (Thermo Scientific, USA). Gene expression was analysed quantitatively by use of the 7500 Real-Time PCR system (Applied Biosystems, Life Technologies, USA). The primers and probes for CK5, CK14, CK8 and CK18 were designed on the basis of published gene sequences (NCBI and PubMed). β-actin was a loading control (Supplementary Table.1).

***In vivo* examination of sweat gland formation**

To testify the tissue-forming capability of 3D-ECM mimics, bioprinted samples (3 ×3mm) of 6 groups (the same groups as previous design) were transplanted into the burned paws of wild-type C57/B16 mice. Before transplantation, mice were anesthetized with 2% isoflurane and then one hindpaw of each mouse was held in contact with the metal plate (65°C) for 15s. A medical elastic bandages was arranged

on the paw to keep the bioprinted samples remain intact wounds. Mice were allowed to recover from anesthesia in their homecages immediately afterward.

The iodine/starch sweat test was performed after 14 days to evaluate sweat gland–specific function. For the test, animals were immobilized and paws with transplanted material were painted with a solution of 3% (wt/vol) iodine in ethanol. Once dry, a suspension of 40% (wt/vol) starch in mineral oil was painted on the paws; sweat was detected as dark spots. To measure sweat secretion in the footpads, images were taken of mouse paws after the starch-iodine assay, and the number of black dots were counted within 15 minute. Sweat gland formation was also evaluated by immunofluorescence assay and histology.

Statistical analysis

Each experiment was independently performed at least 3 times. Data are expressed as mean ± SD. Data were analyzed by use of SPSS for Windows (SPSS Inc., Chicago, IL, USA) and compared by Student's *t* test. $P<0.05$ was considered statistically significant.

RESULTS

Characterization of bioprinted 3D-ECM

The bioprinting procedure of the cell-laden 3D-ECM is depicted in Figure 1A. Figure 1B shows a cross-sectional view of the same sample. To assess the distribution of cells, fluorescence microscopy of samples was used to visualize GFP-positive cells. Cells were homogeneously embedded in the bioprinted matrices after 24-h cell culture,

whether cross-linked or not (Fig. 1C). Comparatively, cross-linked bioprinted 3D-ECM provided better support for cell spreading and growth and so was used for additional experiments. The structural integrity of the bioprinted 3D-ECM could remain for at least 3 weeks after cross-linking (Supplementary Fig. 1).

We further examined the 3D printed structure and cell attachment in bioprinted 3D constructs after 72-h culture by SEM (Fig. 1D). Various researchers have proposed that printing 3D pore organization plays an important role in cell survivability and ECM deposition. SEM results revealed that the bioprinted 3D constructs possess of the rational pore morphology and architecture as well as reproducibility. Although most cells were embedded in printed hydrogel constructs, some cells were attached and spread out into the designated microholes (Fig. 1D left) and the presence of ECM-like components deposited and interconnected between the microholes of the 3D structure at day 3 of culture (Fig. 1D right). Once began to differentiating to sweat gland cells, epithelial progenitors appeared stretched on the printed scaffolds producing the extracellular matrix, oriented in all directions. Taking into account the incubation period and the evident differentiation stage, presumably, these cells and components might be correspond to epithelial progenitors and ECM. Certainly, they should be confirmed in our further studies.

Cell viability

To achieve a desired number and distribution of cells in the 3D-ECM, high cell viability should be maintained. However, during the 3D printing, the nozzle seemed to generate shear stress to cells and reduce cell viability. So we checked the

cytocompatibility of bioprinted 3D samples after the printing process. The number of active cells in the printed 3D constructs and mixed gel without printing did not differ (Fig. 2A). Intriguingly, cell viability in the printed construct including EGF and dermis homogenates showed significant cell viability after 7 days ($P<0.05$). The cell-printed construct with cells only showed lower cell viability. The bioprinted matrices may cushion cells during extrusion from the nozzle, and EGF and dermis homogenates may promote the viability of cells during their residence in the matrices. Moreover, the cell morphology in the printed construct including EGF and PD homogenates (Eps+PD+EGF group) began crimping and emerging gathered phenomenon, whereas other groups maintained their original morphologic features on day 7 of incubation(Fig. 2B). This phenomenon is commonly only observed in formative sweat gland cells, thus it might be implied that epithelial progenitors began to differentiate into sweat gland cells and acquired the desired sweat gland-like pattern.

BMP-4 expression and growth factors released from bioprinted ECM

Sweat gland formation is derived from epidermal progenitors, whose induction and maintenance requires a possible signal from the PD. To validate this possibility, we examined different regional dermis for BMP-4 expression, released from dermal components as a potent epidermal inducer (Fig. 2C). The protein level of BMP-4 was higher in PD than DD homogenates. PD homogenates in bioprinted 3D constructs may favor sweat glandular cell fates [16].

To assess the bioactivity of EGF and BMP-4 delivered by bioprinted 3D-ECM

mimics, we determined EGF and BMP-4 secretion at different times. BMP-4 was released slower from PD homogenate-incorporated bioprinted 3D constructs than controls, with less BMP-4 release from DD homogenate-incorporated constructs (Fig. 2D) ($P<0.05$). The cumulative release profiles of EGF showed a prolonged and gradual release for at least 1 week (Fig. 2E). Thus, the bioprinted 3D mimics are a suitable system for EGF and BMP-4 delivery to induce cell differentiation. Use of this bioprinted 3D construct permitted the restriction in the formation of integrated cellular clustering matrices and the diffusion of soluble factors within designed geometries of the micropatterned ECMs.

3D-ECM induces sweat gland differentiation of epidermal progenitors *in vitro*

Epidermal progenitors routinely maintain the main epidermal markers CK5 and CK14 (representing the primary CKs of stratified epithelia). Once the cells differentiate into sweat gland cells, they should lose the basic epithelial markers (CK5, CK14) and gain luminal epithelial markers (CK8, CK18) [4] (Supplementary Fig. 2). In this regard, a conversion of markers may serve as a differentiation indicates in this study.

Immunofluorescence staining confirmed the progression of early epidermal differentiation. To induce epidermal cell development, we cultured 3D-ECM for 14 days; most cells were positive for CK8 and CK18 in the 3D-ECM samples incorporating EGF and PD (Eps+PD+EGF group) (Fig. 3A). With culture, both CK8 and CK18 remained coexpressed. However, without EGF, differentiation decreased (Eps+PD group). Undifferentiated cells cultured in 3D-ECM samples incorporating EGF and DD maintained the expression of CK5 and CK14 (Eps+DD+EGF group). In

support of the immunofluorescence studies, we detected the mRNA expression of epidermal differentiation markers CK8 and CK18 (Eps+PD+EGF group) ($P<0.05$) (Fig. 3B). With or without EGF, DD components in 3D-ECM (Eps+DD+EGF group, Eps+DD group) could not promote epidermal cell differentiation to sweat gland lineages as compared with PD components (Eps+PD+EGF group). Thus, epidermal progenitors in the 3D-ECM samples acquired a favorable environment to mimic their natural fate-determination niche.

3D-ECM leads sweat gland regeneration *in vivo*

In mice, sweat glands are restricted to foot paw pads, so the *in vivo* model system should be well established and accessible for evaluating sweat gland regeneration. To determine whether 3D-ECM could lead to sweat gland regeneration *in vivo*, we performed an iodine/starch-based sweat test on burned paws of mice at day 14 after 3D-ECM implantation. When starch was painted on the paws, only mice with 3D-ECM incorporating EGF and PD (Eps+PD+EGF group) showed individual sweat glands (represented by black dots on foot pads) appeared and the number increased within10 minutes; however, no obvious black dot was observed in other groups even after 15 minutes (Fig. 4A). Presumably, only paws of mice with 3D-ECM incorporating EGF and PD (Eps+PD+EGF group) restored sweat gland function. By contrast, other groups showed macroscopically healed wounds but failed to sweat.

In this study, GFP-expressing cells were bioprinted with 3D-ECM to track the cells in the regenerating sweat glands. The skin of mouse paws was harvested on day 14 after surgery and examined by fluorescent microscopy. Tissues were stained with

DAPI to reveal cell distribution in the tissue. Fluorescence imaging of GFP-positive cells were visible more or less in all groups, but the efficient epithelial differentiation into sweat glands appeared only in wounds of the groups treated with 3D-ECM incorporating both EGF and PD (Eps+PD+EGF group) (Fig. 4B); without either of these factors, only sporadic differentiation occurred. A large number of GFP-labeled cells were visible in the stratified epidermis of groups treated with 3D-ECM incorporating both EGF and DD (Eps+DD+EGF group). The preliminarily formed sweat gland structure presumably reflects that epithelial differentiation depends on ECM in addition to perhaps a microenvironment produced by the dermis.

We examined wound healing 14 days after treatment by histology (Fig. 4C). The regenerated skin tissue of mouse paws replaced the scarred tissue with bioprinted 3D-ECM treatment. The tissue-forming capability of 3D-ECM samples was better with EGF and dermis than other treatments. These observations highlight the cell growth capabilities of our cell-printed constructs including EGF and dermis homogenates. Notably, sweat glands occurred in the newly formed skin with 3D-ECM incorporating EGF and PD (Eps+PD+EGF group). Histology results also indicate total degradation of the 3D-ECM samples *in vivo*.

DISCUSSION

We used bioprinting technology to create a functional *in vitro* cell-laden 3D-ECM mimics with composite hydrogels based on gelatin and sodium alginate for mimicing the chemical and physical ECM environments. To achieve effective specific

differentiation, mouse PD and EGF were synchronously incorporated into the 3D-ECM mimics to create the inductive niche for epidermal progenitors. The developed biological 3D construct could maintain cell viability, thereby facilitating cell spreading and matrix formation. *In vitro*, the bioprinted 3D-ECM mimics could effectively impose a restrictive niche for epidermal progenitors that ensures unilateral differentiation into sweat gland cells. Furthermore, direct delivery of bioprinted 3D-ECM mimics into burned paws of mice resulted in functional restoration of sweat glands. This study represents the rational design to enhance the specific differentiation of epidermal lineages and may have clinical and translational implications in regenerating sweat glands.

Various attempts have been made to improve the feasibility and applicability of regenerating sweat glands in the clinic; however, effective and optimal methods have not yet been well developed [20]. The emergence of bioprinting technology seems to provide a favorable tool to meet the demands of tissue engineering and regenerative applications. By comparison, the conventional techniques used to manufacture scaffolds evidently have several limitations, particularly the lack of full control of the pore morphology and architecture as well as reproducibility [19]. Despite numerous studies on 3D printing technology for tissue regeneration, no study has coupled the bioprinting design with specific differentiation for regenerating sweat glands, which has health implications. In the present study, besides the material (including PD and EGF components within it) itself with the primary responsibility for the biological effects on epithelial progenitors, 3D printed structure enable the fabrication of ECM

with enhanced accuracy and reproducibility of the internal architecture (e.g., porosity, pore size, spatial distribution, and interconnectivity of pores) thereby propelling cell growth, facilitating cell spreading and matrix formation. Another important role of 3D printing is the feasibility of including living cells and inductive molecules simultaneously during fabrication without the limitation of time and culture conditions. In contrast to common cell culture and then transplantation, the designed 3D bioprinted ECM for sweat gland regeneration, on enhancing specific differentiation of epidermal lineages, offers a direct and effective strategy that may be a therapeutic tool for translational application.

Theoretically, regeneration by cell differentiation is not unique to 3D printing technology. However, maintenance of high cell density and feasibility of *in situ* organized printing are overwhelming advantages over other cell delivery approaches [21,22]. The present study demonstrated high cell viability during the printing process, which is further corroborated by the tissue-formation capabilities during subsequent transplantation. This finding can be explained by the cushion and promoting-growth function of our printing ECM mimics. Further, typical of all multipotential cells, transplantation of epidermal progenitors must rely on ECM for differentiation into a specific tissue. Our *in vitro* and *in vivo* data confirmed the previous speculation of a gland lineage–inductive power from adult dermal components as embryonic tissue for regenerating sweat glands [4, 7].

Adult basal epithelial stem cells, namely epidermal progenitors, have been identified as important players in generation and maintenance of skin tissues [23].

Meanwhile, epidermal stem cell differentiation relies on an underlying basement membrane enriched in ECM proteins and growth factors[5, 6, 8]. However, the accurate *in vitro* simulation remains difficult at least in part because of the lack of a comprehensive definition of the critical factors of the niche. In mice, sweat glands are restricted to foot pads; adult epithelial progenitors are expected to behave differently in diverse settings [4]. Therefore, mice are attractive models to investigate the underlying mechanism of a sweat gland–induction niche and to the possibility of guiding cell fate in a highly restrictive microenvironment. The initial data from our study suggest that dorsal progenitors within the bioprinted 3D constructs containing PD components and EGF could differentiate into sweat gland cells by a phenotype conversion from $CK5^+/CK14^+$ to $CK8^+/K18^+$. In contrast, dorsal progenitors within an ECM without PD faithfully maintained the $CK5^+/CK14^+$ phenotype. Our findings were also intriguing given the well-documented importance of BMP-4 released from DD or PD in dictating an epithelial differentiation lineage [17, 18]. Another point from our study is that even though EGF plays a key role in developing skin appendages [24], it cannot be considered a single inducer for sweat gland differentiation. Overall, this study enlarges the understanding that epidermal progenitors can switch their phenotype to sweat gland lineages in a spatially inductive niche and corroborates that EGF coupling with dermal components is a potent inducer for fate determination.

Despite *in vitro* evidence, *in vivo* functional regeneration after transplantation is deemed to be the better judgment for translational clinical application. The *in vivo*

model should be suitable for evaluating and characterizing sweat gland function. Using the iodine/starch sweat test, we observed a near-complete loss of sweat function in burned paws of mice. As expected, the designed bioprinted mimics could achieve functional regeneration or restoration of sweat glands. No previous reports have shown such a fast functional regeneration of sweat glands, although some studies have shown some healing by gene-correction therapy during pregnancy [25]. Our previous research has also shown that the feasibility of sweat gland regeneration by tissue engineered approaches, but it needs a relatively long-term process [26]. Combined with strong evidence from *in vitro* culture, these findings support that this instruction conveyed through bioprinted 3D-ECM mimics facilitates the directed differentiation of epithelial progenitors to sweat gland lineages. Although further work is required to dissect the molecular mechanisms, a bioprinted 3D-ECM mimics is an attractive option that opens up new avenues for tissue reconstruction.

CONCLUSION

In summary, we describe a feasible method to fabricate bioprinted 3D-ECM mimics that provides the spatial cues to determine cell-differentiating behavior. Bioprinting provides a new efficient route to deliver cells in a fast, accurate, "off-the-shelf" manner, facilitating quick application in the clinic, which is critical for large-scale deep burns or other wounds. Collectively, our *in vitro* and *in vivo* data underscore the capabilities of bioprintable microenvironmental factors that impact the behavior and fate specification of adult epidermis progenitors during sweat gland regeneration. The

reproducible 3D-ECM mimics may offer insights into broad translation for regeneration of other tissues by re-creating the representative microenvironmental characteristics for an inductive niche.

Acknowledgements

This paper was supported in part by the National Nature Science Foundation of China (81121004, 81230041, 81372066 and 8157080212) and the National Basic Science and Development Program (973 Program, 2012CB518105).

Author contributions

S.H. was responsible for the design and primary technical process, conducted the experiments, collected and analyzed data, and wrote the manuscript. B.Y. helped perform the main experiments and helped with the surgical design of the animal model. J.X. participated in cell experiments, animal surgeries, and post-op animal care. S.H. and X.F. collectively oversaw the collection of data and data interpretation, and revised the manuscript.

Competing interest statement

The authors declare that they have no competing financial interests.

References

[1] W.C. Jr. Lobitz, and R.L. Dobson, Dermatology: the eccrine sweat glands, Annu. Rev. Med.12(1961)289–298.

[2] W.P. Cheshire, R. Freeman, Disorders of sweating, Semin. Neurol. 23(2003)399–406.

[3] X.B. Fu, T.Z. Sun, X.K. Li, Z.Y. Sheng, Morphological and distribution characteristics of sweat glands in hypertrophic scar and their possible effects on sweat gland regeneration, Chin. Med. J.118(2005)186– 191.

[4] C.P. Lu, L. Polak, A.S. Rocha, H.A. Pasolli, S.C. Chen, N. Sharma, C. Blanpain, E. Fuchs, Identification of stem cell populations in sweat glands and ducts reveals roles in homeostasis and wound repair, Cell. 150(2012) 136-150.

[5] T. Shikiji, M. Minami, T. Inoue, K. Hirose, H. Oura, S. Arase, Keratinocytes can differentiate into eccrine sweat ducts in vitro: Involvement of epidermal growth factor and fetal bovine serum, J. Dermatol. Sci.33(2003)141–150.

[6] C. Ferraris, G. Chevalier, B. Favier, C.A. Jahoda, D. Dhouailly, Adult corneal epithelium basal cells possess the capacity to activate epidermal, pilosebaceous and sweat gland genetic programs in response to embryonic dermal stimuli, Development.127(2000) 5487–5495.

[7] T. Biedermann, L. Pontiggia, S. Bo¨ttcher-Haberzeth, S. Tharakan, E. Braziulis, C. Schiestl, M. Meuli, E. Reichmann, Human eccrine sweat gland cells can reconstitute a stratified epidermis, J. Invest. Dermatol.130(2010)1996–2009.

[8] M.A. Deugnier, M.M. Faraldo, B. Janji, P. Rousselle, J.P. Thiery, M.A. Glukhova, EGF controls the in vivo developmental potential of a mammary epithelial cell line possessing progenitor properties, J. Cell. Biol. 159(2002) 453-463.

[9] M.P. Lutolf, P.M. Gilbert, H.M. Blau, Designing materials to direct stem-cell fate, Nature. 462(2009)433-441.

[10] F.P.W Melchels, M.A.N. Domingos, T.J. Klein, J. Malda, P.J. Bartolo, D. Hutmacher, Additive manufacturing of tissues and organs. Progress in Polymer Science. 37(2012)1079-1104.

[11] A. Berner, M.A. Woodruff, C.X. Lam, M.T. Arafat, S. Saifzadeh, R. Steck, J. Ren, M. Nerlich, A.K. Ekaputra, I. Gibson, D.W. Hutmacher, Effects of scaffold architecture on cranial bone healing. Int. J. Oral. Maxillofac. Surg. 43(2014):506-513.

[12] A. Mata, Y. Geng, K.J. Henrikson, C. Aparicio, S.R. Stock, R.L. Satcher, S.I. Stupp, Bone regeneration mediated by biomimetic mineralization of a nanofiber matrix. Biomaterials.31(2010):6004-6012.

[13] R.N. Shah , N.A. Shah , M.M. Del Rosario Lim , C. Hsieh , G. Nuber , S.I. Stupp, Supramolecular design of self-assembling nanofibers for cartilage regeneration. Proc. Natl. Acad. Sci. U S A. 107(2010):3293-3298.

[14] C.D. Stern, Neural induction: Old problem, new findings, yet more questions, Development.132(2005)2007–2021.

[15] T. Tumbar, G. Guasch, V. Greco, C. Blanpain, W.E. Lowry, M. Rendl, and E. Fuchs, Defining the epithelial stem cell niche in skin, Science.303(2004)359–363.

[16] M. Plikus, W.P. Wang, J. Liu, X. Wang, T.X. Jiang, C.M. Chuong, Morpho-regulation of ectodermal organs: Integument pathology and phenotypic variations in K14-Noggin engineered mice through modulation of bone morphogenic protein pathway, Am. J. Pathol.164(2004)1099– 1114.

[17] V. A. Botchkarev, A. A. Sharov, BMP signaling in the control of skin development and hair follicle growth, Differentiation. 72(2004)512–526.

[18] M. Pummila, I. Fliniaux, R. Jaatinen, M.J. James, J. Laurikkala, P. Schneider, I. Thesleff, M.L. Mikkola, Ectodysplasin has a dual role in ectodermal organogenesis: Inhibition of Bmp activity and induction of Shh expression, Development.134(2007)117–125.

[19] X. Wang, Y. Yan, Y. Pan, Z. Xiong, H. Liu, J. Cheng, F. Liu, F. Lin, R. Wu, R. Zhang, Q. Lu, Generation of threedimensional hepatocyte/gelatin structures with rapid prototyping system, Tissue Eng. 12(2006)83–90.

[20] P. Martin, Wound healing--aiming for perfect skin regeneration, Science. 276(1997) 75-81.

[21] I. T. Ozbolat, Y. Yu, Bioprinting toward organ fabrication: challenges and future trends, IEEE Trans. Biomed. Engineering 60(2013)691-699.

[22] S. V. Murphy, A. Atala, 3D bioprinting of tissues and organs, Nature biotechnology. 32(2014)773-785.

[23] Y. Wang, S. W. Hayward, M. Cao, K. Thayer, G. Cunha, Cell differentiation

lineage in the prostate, Differentiation. 68(2001)270-279.

[24] G. A. Vargas, E. Fantino, C. George-Nascimento, J. J. Gargus, H. T. Haigler, Reduced epidermal growth factor receptor expression in hypohidrotic ectodermal dysplasia and tabby mice, J. Clin. Invest 97(1996) 2426-2432.

[25] A. K. Srivastava, M. C. Durmowicz, A. J. Hartung, J. Hudson, L. V. Ouzts, D. M. Donovan, C. Y Cui, D. Schlessinger, Ectodysplasin-A1 is sufficient to rescue both hair growth and sweat glands in Tabby mice, Hum. Mol. Genet. 10(2001)2973– 2981.

[26] Huang S, Xu Y, Wu C, Sha D, Fu X. In vitro constitution and in vivo implantation of engineered skin constructs with sweat glands, Biomaterials. 31(2010)5520-5525.

Figure legends

Figure 1. Characterization of bioprinted 3D extracellular matrix (3D-ECM). (A) Schematic of the printing process with epidermal progenitors and ECM incorporated in composite hydrogels. (B) Representative images of the cell-laden printed construct. (C) Fluorescence images of cells homogeneously embedded in the bioprinted matrices after 24-h cell culture. (D) Scanning electron microscopy of epidermal progenitors that had attached and spread out into the designated microholes (left: Bar=500μm, 100μm) and the presence of ECM-like components deposited and interconnected between the microholes at day 3 of culture (right: Bar=500μm, 100μm).

Figure 2. Cell viability and growth factor delivery of 3D-ECM *in vitro*. (A) Cytocompatibility of bioprinted 3D-ECM samples after the printing process. (B) Cell morphology of bioprinted 3D-ECM samples after 7 days of culture (scale bar, 200 μm). (C) Western blot analysis of bone morphogenic protein 4 (BMP-4) protein expression from plantar and dorsal dermal homogenate. (D) BMP-4 and (E) epidermal growth factor (EGF) release from bioprinted 3D-ECM samples over time. *P< 0.05. PD, plantar dermis; DD, dorsal dermis

Figure 3. 3D-ECM mimics induce sweat gland differentiation of epidermal progenitors *in vitro*. (A) Immunofluorescence analysis of differentiation into sweat gland–specific lineages after 2 weeks of culture. Cell nuclei were stained with DAPI. A total of 5 replicates were tested, with representative images selected (scale bar, 50 μm). (B) Gene expression of differentiation into sweat gland–specific lineages after

2-week culture. Data are mean±SD (n=5) normalized to β-actin, and relative to the control. *P< 0.05.

Figure 4. 3D-ECM mimics lead to sweat gland regeneration *in vivo* in mice. (A) Iodine/starch-based sweat test on paws of mice at day 14 after surgery (dark spots on foot paw pads are positive; only in Eps+PD+EGF group). (B) Fluorescence imaging of GFP-positive cells and epithelial differentiation into sweat glands in wounds of mice at 14 days after 3D-ECM mimics implantation. The tissues were stained with DAPI to reveal cell distribution in tissue (scale bar, 50 μm). (C) Histology of wound healing in mouse paws at 14 days after 3D-ECM mimics implantation (scale bar, 200 μm).

List of Supplementary Materials

Supplementary Fig. 1. Fluorescence images of the structural integrity of the bioprinted 3D-ECM after cross-linking (scale bar, 200 μm).

Supplementary Fig. 2. (A) Double immunofluorescence staining of epidermal progenitors of dorsal skin with anti-K5 and K14 antibodies (for main epidermal markers CK5 and CK14, respectively). (B) Double immunofluorescence staining of epidermal progenitors of plantar skin with anti-K8 and K18 antibodies (for luminal epithelial markers CK8 and CK18, respectively) (scale bar, 50 μm).

Supplementary Table.1.

The following oligonucleotides were used as PCR primers:

K5: Forward: 5'- GATGCCAGAAACAAGCTGACAGAG-3'

and Reverse: 5'- ACACTTAGCCCGCTACCCAAAC-3'

K14: Forward: 5'-CCCACTGAGATCAAAGACTACAGCC-3'

and Reverse: 5'-TCTCCGCCATCTTCTCGTACTGA-3'

K8: Forward: 5'- CTCACTAGCCCTGGCTTCAG-3'

and Reverse: 5'- ACAGCTGTCTCCCCGTGA-3'

K18: Forward: 5'-TGTGACATCTTCCCTCTTCTCC-3'

and Reverse: 5'-TTCAACATGGGCACCAATAAAG-3'

β -actin: Forward: 5'-GTGGGCCGCTCTAGGCACCA-3'

and Reverse: 5'-TGGCCTTAGGGTTCAGGGGGG-3'